

# Self-Powered RF Sensor Antenna for Implantable and Ingestible Medical Devices

# Abhishek Kumar Saroj<sup>1</sup>, Ravi Mali<sup>2</sup>, Praveen Singh Rathore<sup>3</sup>, Ajitesh<sup>4</sup>, Manoj Kumar Meshram<sup>5</sup>

Department of Electronics Engineering, IIT (BHU) Varanasi, UP, India.

E-mail: ¹abhisheksaroj1988@gmail.com, ¹abhisheksaroj.srf.ece23@itbhu.ac.in

#### **Abstract**

Radio frequency (RF) devices such as antennas play a crucial role in implantable and ingestible medical devices (IMDs) by enabling wireless communication, energy harvesting, and localization links between transmitter (Tx) and receiver (Rx). Implantable and ingestible medical devices (IMDs) have transformed modern healthcare by enabling real-time monitoring and improving treatment outcomes. Radio frequency (RF) sensor antennas are key components in these devices and are widely used in biomedical applications for early diagnosis, treatment, and continuous health monitoring. RF-enabled IMDs monitor vital parameters such as temperature, blood pressure, glucose levels, oxygen saturation, pH, and blood composition. These antennas also support devices like pacemakers and defibrillators in managing cardiac conditions. In addition to human healthcare, they are applied in animal health monitoring and veterinary diagnostics. Implanted antennas detect physiological changes and wirelessly transmit data to external processing units, allowing real-time access for medical experts. This integration of RF sensing in IMDs enhances the ability to detect diseases early and deliver timely interventions, making them essential tools in both clinical and remote healthcare settings. This article presents two RF sensor antennas—FR-4 integrated (Ant-1) and miniaturized helical (Ant-2)—designed for implantable and ingestible medical devices, particularly in veterinary applications, operating in the 400–500 MHz range. Ant-1 is fabricated on an FR-4 substrate ( $51 \times 28 \times 1.6 \text{ mm}^3$ , Er = 4.4,  $\tan \delta = 0.002$ ), resonating at 434 MHz with a bandwidth of 32.13 MHz and a total gain of approximately -36.92 dB without the phantom model and with the phantom in an acceptable range. Ant-2 is a miniaturized normal-mode helical antenna made of 0.9 mm diameter copper wire, also resonating at 434 MHz and both antennas integrate a surface acoustic wave (SAW) sensor to enhance wireless sensing. SAW

sensors utilize acoustic waves on piezoelectric surfaces to detect parameters like temperature, pressure, strain, and displacement, enabling real-time, wireless physiological monitoring in biomedical applications.

**Keywords:** Radio Frequency (RF), Transmitter (Tx), Receiver (Rx), Implantable and Ingestible Medical Devices (IMDs), FR-4 (Flame Retardant Grade-4), Surface Acoustic Wave (SAW).

#### 1. Introduction

Antennas play a key role in transmitting information through wireless communication by establishing links between implantable and ingestible devices, diagnostic imaging sensors, biosensing devices, and biotelemetry equipment. Designing biomedical RF devices requires numerous trials, including miniaturization and integration into compact devices, ensuring biocompatibility with the human body and animals, conforming to biological structures, accounting for signal attenuation and propagation in the body, optimizing power efficiency, mitigating electromagnetic interference (EMI), and ensuring compliance with regulatory standards. Solving these challenges necessitates expertise in the biomedical antenna field and experimental verifications. Today, health and a healthy lifestyle have become primary concerns for human beings since the COVID pandemic. Therefore, healthcare monitoring systems desperately need to adopt the use of RF-enabled smart biocompatible devices and telemetric systems to monitor, diagnose, and provide treatment to patients [1]. The basic parameters of conventional antennas depend on geometry, size, material, and performance parameters such as gain, bandwidth, efficiency, and impedance. These radio antennas have a widespread range of applications that include modern mobile communication (3G, 4G, 5G, 6G technologies), wireless local area networks (WLAN), IoT (Internet of Things), Bluetooth, radio frequency identification (RFID), advanced power management systems (APMS), defense, and healthcare industries [2-4]. In healthcare industries, wireless medical devices (WMD) are placed inside or outside the human body to realize numerous sensing and stimulating functionalities for diagnosis. A critical literature review analysis is conducted focusing on three types of in-body medical devices: (1) devices that are implanted inside or outside the human body, known as implantable devices; (2) devices that are ingested like regular pills, known as ingestible devices; and (3) devices that are injected into the human body via needles, known as injectable

devices, such as pacemakers, artificial joints, capsule endoscopy, and smart pills for drug delivery systems, etc. [5]-[8]. The same procedures are also applied for animal disease diagnosis and treatments [9]-[13].

In this article, radio frequency sensor antennas are presented and compared with two dissimilar antennas named Ant-1 (Microstrip Patch Antenna) and Ant-2 (Normal Mode Helical Antenna). Ant-1 has a planner structure, whereas Ant-2 has a non-planar structure; both antennas have different radiating properties. These antennas are designed for the study of implantable and ingestible biomedical devices (IMDs) used in the diagnosis and treatment of animals and humans. Ant-1 and Ant-2 are loaded with surface acoustic wave sensors to work in a standalone and passive environment [14]-[16]. The proposed RF sensor-enabled antennas operate without an internal power source, meaning they function in a passive, power-free condition. They require RF energy of a specific frequency to activate. The antennas are triggered when signals of the desired frequency are received. In this study, a 434 MHz ISM band signal is used to analyse the performance of Ant-1 and Ant-2. Furthermore, the analysed data and results are presented in the respective sections. The specific absorption rate (SAR) analysis of the antenna configuration has also been considered and reviewed [17]-[18]. This article is structured as follows: The Introduction outlines the key concepts of the manuscript; the Antenna Design section describes the antenna structure; and the Results section discusses various aspects of the antenna's performance, followed by the Conclusion. Additionally, SAR analysis is conducted using a single-layer muscle phantom model. Specific Absorption Rate (SAR) is a measure of the rate at which energy is absorbed by the human body when exposed to an electromagnetic (EM) field. It is expressed in units of watts per kilogram (W/kg) and quantifies the amount of RF (radio frequency) energy deposited in biological tissues. SAR is especially important for evaluating the safety of wireless devices like mobile phones, wearable electronics, and implantable biomedical antennas, since excessive EM absorption can cause tissue heating or other biological effects [19]-[20]. Standard Regulatory SAR Limits are given in Table 1. These values are averaged over the given mass of tissue (1g or 10g), typically measured over 6 minutes of exposure.

Table 1. SAR Standards

Regulating Body	Averaging Mass	SAR Limit
IEEE / FCC (USA)	1 gram	1.6 W/kg
ICNIRP (Europe/Global)	10 grams	2.0 W/kg

# 2. Antenna Design

The proposed article presents two different RF sensor antennas, named Ant-1 and Ant-2, designed for ISM band applications, as shown in Figure 1. Ant-1 is implemented on an FR-4 substrate with dimensions of  $51\times28\times1.6$  mm³, a dielectric constant of 4.4, and a loss tangent (tan $\delta$ ) of 0.002. FR-4 is selected due to its wide availability and low cost. In the proposed design, traces are made of copper material.

Copper is widely used in biomedical antenna prototyping due to its high electrical conductivity (about 5.76×10<sup>7</sup> S/m), which helps maintain high radiation efficiency and minimize conductor losses a critical factor in electrically small antennas. Although copper is not inherently biocompatible, in our study it is intended for simulation and proof-of-concept purposes. In practical implantable systems, copper traces would be encapsulated in biocompatible layers (e.g., parylene-C, PDMS, or medical-grade silicone), which prevents direct tissue contact [21-22]. The detailed parametric design of Ant-1 is illustrated in Figure 2.

Ant-2 is a helical-type antenna designed to operate at 434 MHz. It is fabricated using copper wire with a diameter of 0.9 mm and a pitch of 1.5 mm. The proposed antennas are analyzed under both open environment conditions and within a closed phantom model using HFSS antenna simulation software, as described in the respective section. The geometrical structure of Ant-2 is shown in Figure 3. Ant-2 operates in the normal mode and is therefore categorized as a normal mode helical antenna (NMHA).

This type of antenna functions when the helix circumference is much smaller than the wavelength ( $C \ll \lambda$ ) and the antenna length is a fraction of the wavelength ( $L \ll \lambda$ ). In this mode, it behaves like a short dipole and radiates linearly polarized waves broadside to the helix axis. Ant-2 is mounted on a  $10\times10$  mm<sup>2</sup> FR-4 substrate with a thickness of 1.6 mm, as shown in Figure 3.

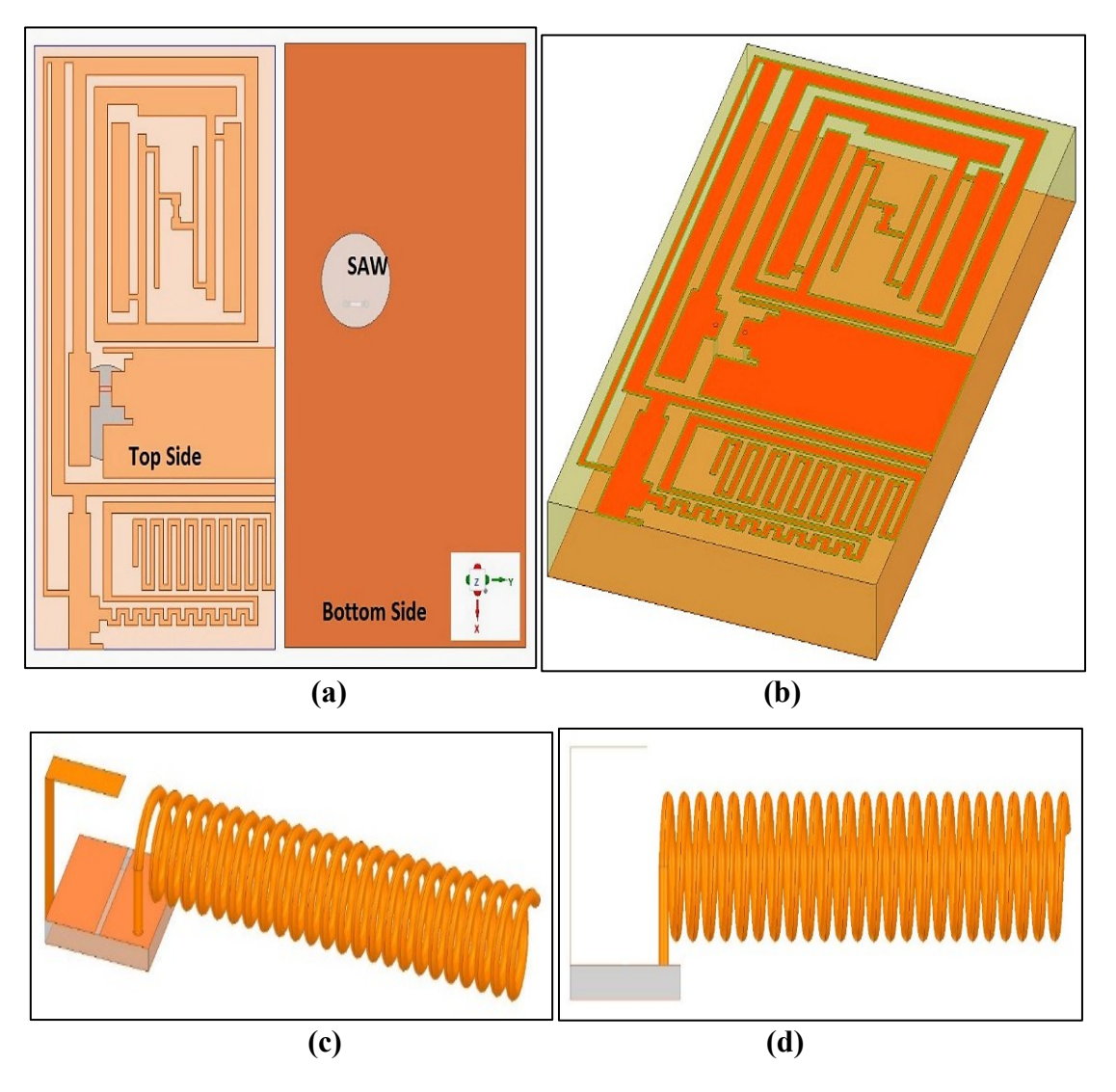


**Figure 1.** Proposed Antenna for Bio-Medical Applications: **(a)** Ant-1 Top and Bottom View, **(b)** Ant-1 Three-Dimensional View, **(c)** Ant-2 Helical Antenna, and **(d)** Ant-2 Side View.

It features several tuning parameters such as wire length, wire diameter, pitch, pitch angle, and helix diameter, which are used to enhance performance. However, it also faces certain limitations, including low gain, narrow bandwidth, low efficiency, and polarization constraints.

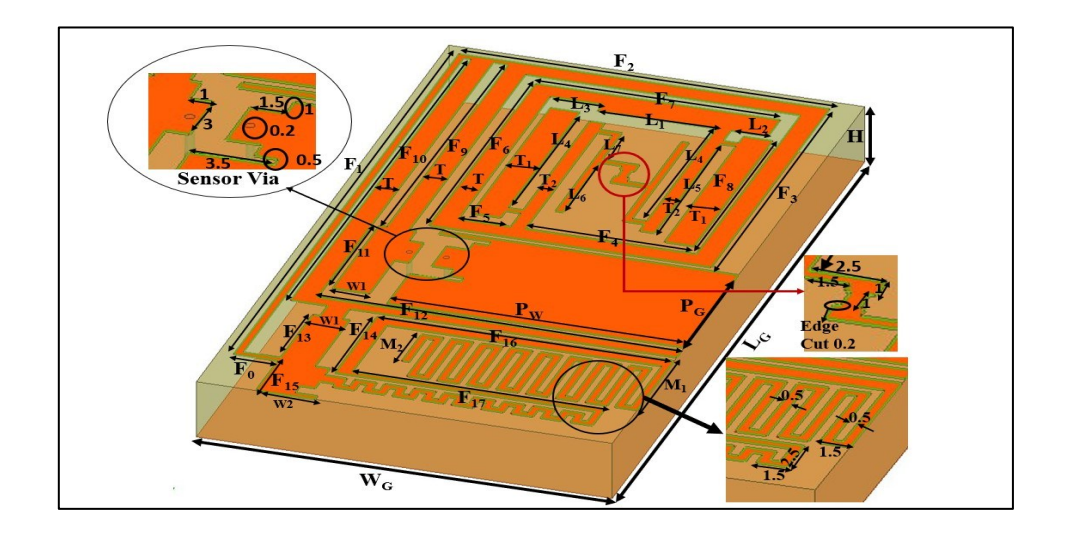


**Figure 2.** Geometrical Details of Ant-1 for Bio-Medical Applications (All the Dimensions are in mm): (W<sub>G</sub>=28, L<sub>G</sub>=51, H=1.6, F<sub>0</sub>=3, F<sub>1</sub>=45.5, F<sub>2</sub>=25, F<sub>3</sub>=24, F<sub>4</sub>=11.5, F<sub>5</sub>=3.5, F<sub>6</sub>=21.5, F<sub>7</sub>=16.5, F<sub>8</sub>=16, F<sub>9</sub>=24.5, F<sub>10</sub>=36.5, F<sub>11</sub>=9.5, F<sub>12</sub>=24.5, F<sub>13</sub>=6.5, F<sub>14</sub>=8.5, F<sub>15</sub>=4.5, F<sub>16</sub>=20, F<sub>17</sub>=17, P<sub>W</sub>=20, P<sub>G</sub>=11, M<sub>1</sub>=7.5, M<sub>2</sub>=4, w1=2.5, w2=4, T=1.5, T<sub>1</sub>=2, T<sub>2</sub>=1, L<sub>1</sub>=8, L<sub>2</sub>=2.5, L<sub>3</sub>=3.5, L<sub>4</sub>=14.5, L<sub>5</sub>=13.5, L<sub>6</sub>=7.5, L<sub>7</sub>=4, Width of Minimum Trace is 0.5).

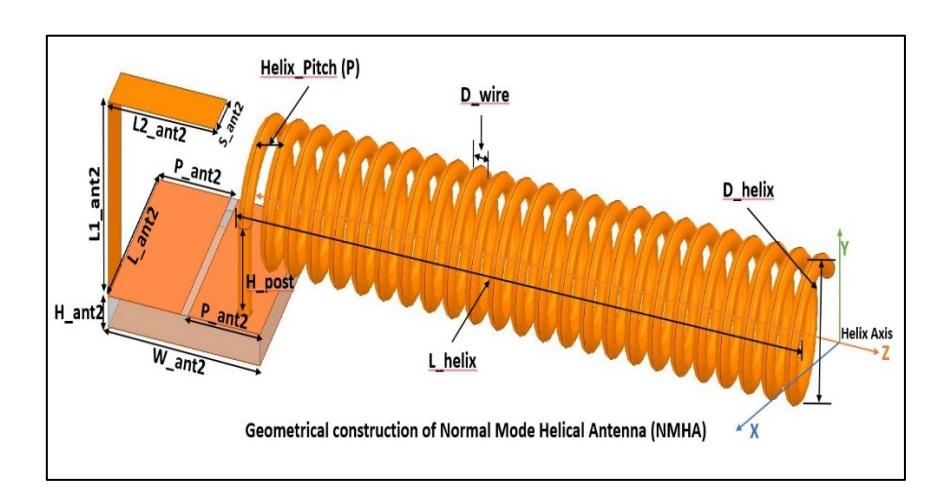
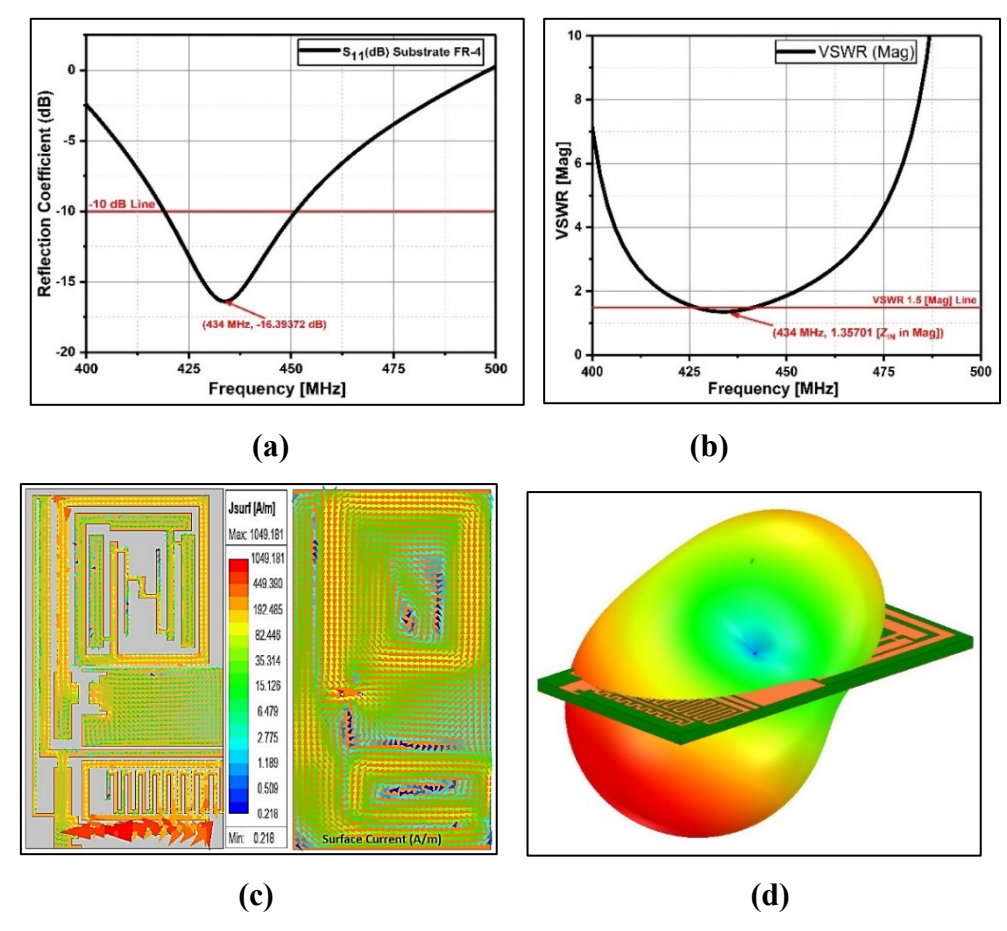


Figure 3. Parametric of Ant-1 for Bio-Medical Applications in millimetre (mm): (L\_ant2=10, W\_ant2=10, P\_ant2=4.5, H\_ant2=1.6, L1\_ant2=10, L2\_ant2=7, S\_ant2=2.5, H\_post=5, P=1.5, D=9, D\_helix=10, L\_helix=35)

# 3. Results and Analysis

The analysed results of antenna (Ant-1) are shown in Figure 4. Figure 4 presents the reflection coefficient (in dB), voltage standing wave ratio (VSWR in magnitude), surface current distribution over the radiating patch and ground (in amperes per meter), and the 3D

radiation pattern of Ant-1, respectively. These results are analysed without using a muscle phantom model. Figure 6 illustrates the investigation results of Ant-1 with the muscle phantom model.

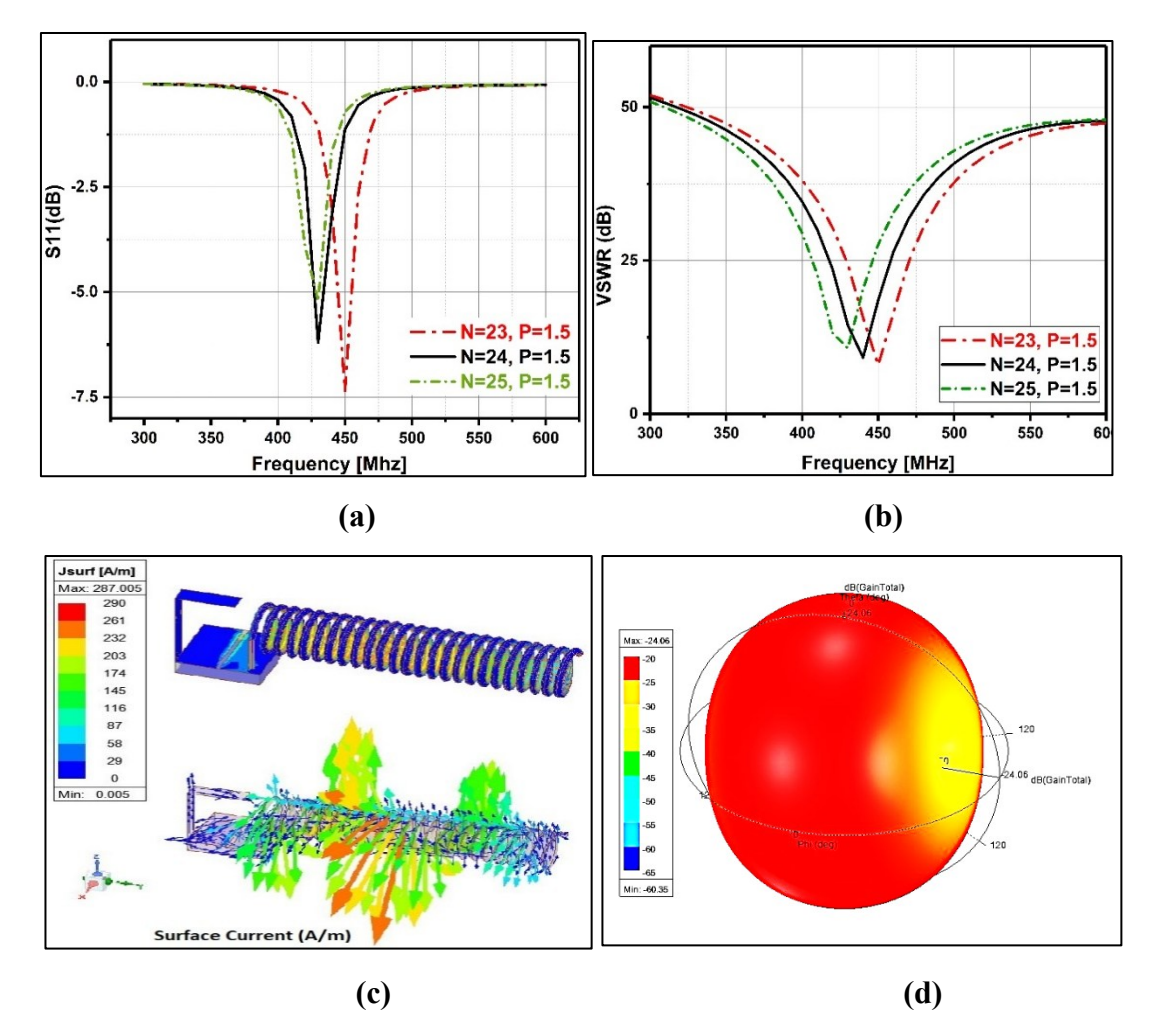


**Figure 4.** Simulation Results of Proposed Ant-1 for Bio-Medical Applications: (a) Ant-1 Reflection Co-efficient in dB, (b) Ant-1 VSWR in Magnitude, (c) Ant-1 Surface Current Distribution Over Radiating Patch and Ground in Amp per Meter, and (d) Radiation Pattern of Ant-1.

The analysed results for Ant-2 are presented in Figure 5. Ant-2 features a helical structure constructed from copper, which functions as the radiating element. Figure 5 displays the reflection coefficient (in dB), voltage standing wave ratio (in dB), current distribution (in vector form, A/m), and gain (in dB) for Ant-2. These results were acquired without utilizing a muscle phantom model, as the high permittivity of body tissues significantly impacts antenna performance. Additionally, since both animal and human phantom models exhibit similar lossy characteristics, the corresponding analysis is illustrated in Figure 6 alongside Ant-1. Table 1 offers a comparative overview of Ant-1 and Ant-2.

**Table 2.** Comparison of Ant-1 and Ant-2

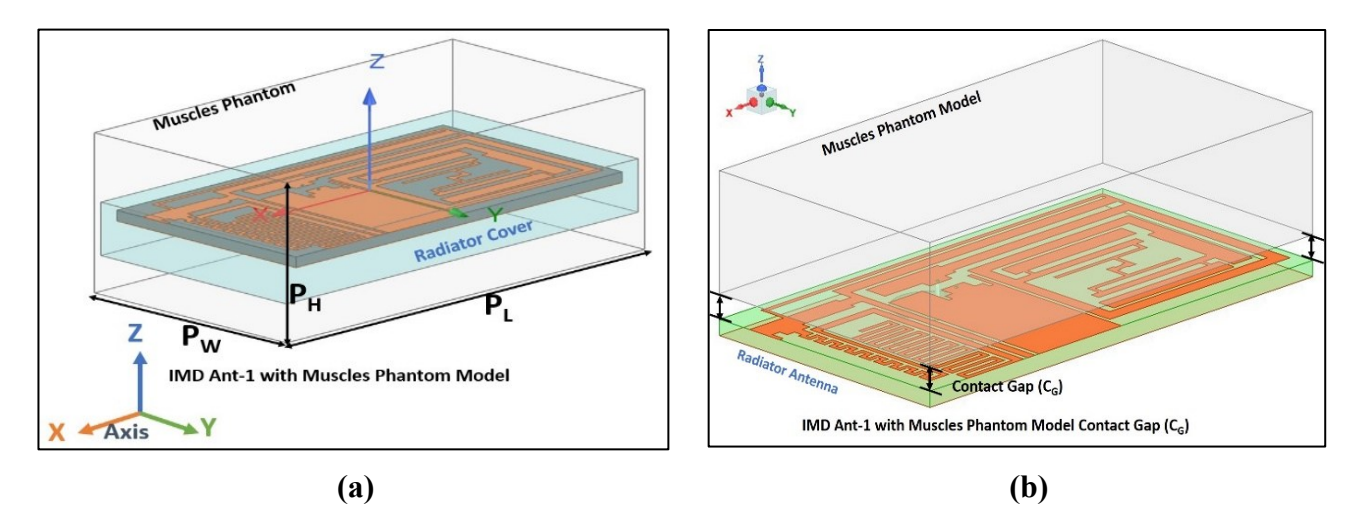
	Antenna Type	Microstrip Patch Antenna (Ant-1)	Helical Antenna (Ant-2)
Simulation	Volume (mm <sup>3</sup> )	28×51×1.6	$\pi \times (0.45)^2 \times 30$
	S <sub>11</sub> (Reflection coefficient)	-16dB	-6.1dB
	≤-6 dB	434 MHz	434MHz



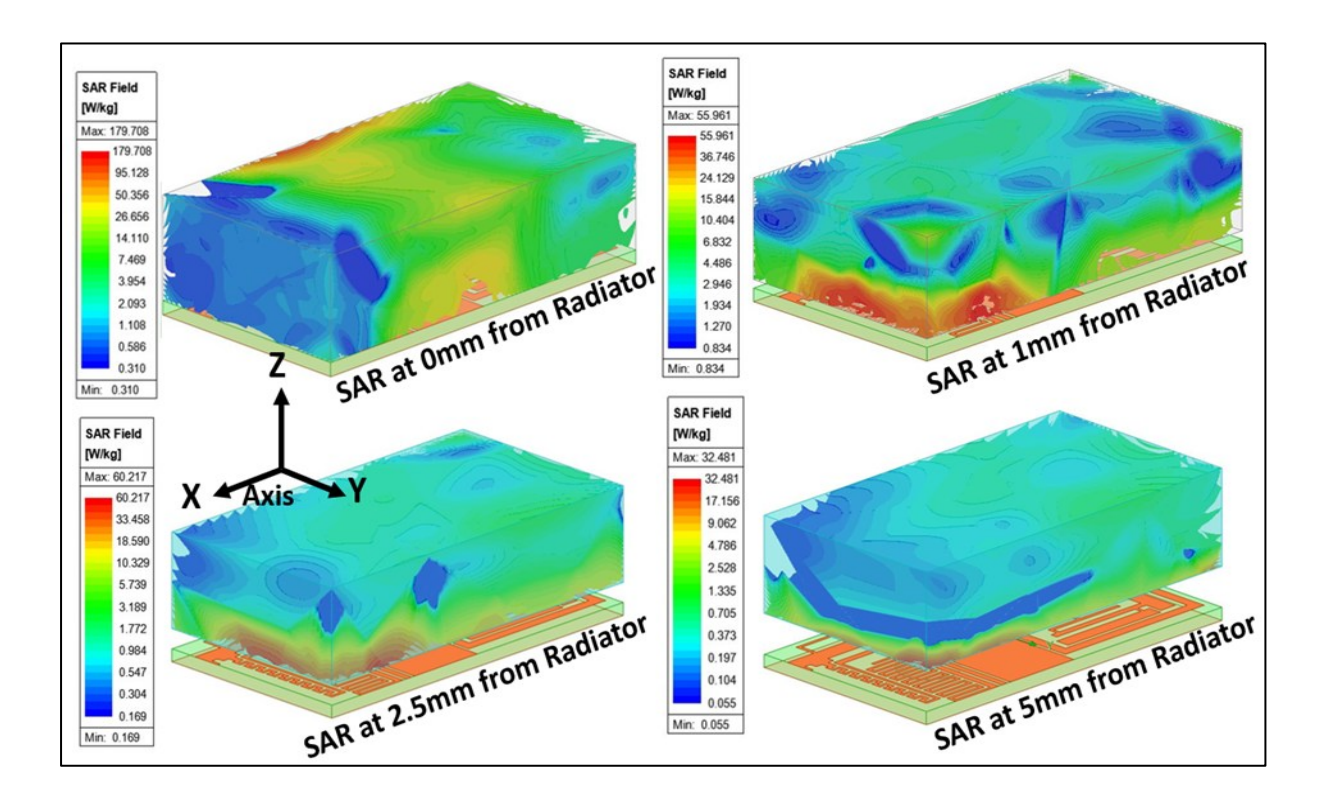
**Figure 5.** Simulation Results of Proposed Ant-2 for Bio-Medical Applications: (a) Ant-2 Reflection Co-efficient in dB, (b) Ant-2 VSWR in dB, (c) Ant-2 Surface Current Distribution Over Radiating Helix in Amp per Meter, and (d) Gain of Ant-2 in dB.

Figure 6 illustrates the simulated analysis of Ant-1 inside the muscle phantom model and outside the phantom model. This mimicking single-layer muscle was designed using dimensions  $P_W = 30$  mm,  $P^L = 56$  mm, and  $P^H = 24$  mm, with permittivity 52.7, relative permeability 1, conductivity 1.73 siemens per meter, and mass density 1050 kg/m³ at a frequency of 2.45 GHz [19]. Figure 6(a) shows that the entire antenna is covered with a PVC

protective cover filled with air, placed inside the muscle phantom model. Figure 6(b) presents the antenna model, which is investigated directly with the muscle phantom model separated by a contact gap. The contact gap (C<sub>G</sub>) refers to the distance between the radiating part of the antenna (Ant-1) and the muscle phantom. The studied SAR analysis is shown in Figures 7 and 8. The simulated SAR value is calculated at various distances measured with respect to the antenna, as shown in Figure 7. Inside the muscle phantom, the SAR value is also studied at a depth of 12 mm, as shown in Figure 8. The parametric analysis of the muscle phantom model's distance with respect to the antenna, in terms of reflection coefficient behavior, is demonstrated in Figure 9. The SAR value is denoted in W/kg, and the transmitted power is set to 1 W for the analysis of the phantom model. It is necessary for the transmitted power to be set such that it must follow defined standard limits for biomedical applications, as mentioned in Table 1. The red dotted line in Figure 9 illustrates that the reflection coefficient (dB) falls within the ISM band when the antenna (Ant-1) is placed inside a 12 mm muscle phantom. Due to the lossy nature of muscle, the resonating frequency of the antenna (Ant-1) is observed and shown in the reflection coefficient curve in Figure 9.



**Figure 6.** Proposed Antenna Ant-1 with Mimicking Muscles Phantom Model: (a) Antenna Inside the Phantom Model with Protective Cover, and (b) Antenna Outside the Phantom Model without Protective Cover and Variable Contact Gap (C<sub>G</sub>).



**Figure 7.** Proposed Antenna Ant-1 with a Mimicking Muscles Phantom Model with Respect to Different Contact Gap (C<sub>G</sub>) as shown in figure caption.

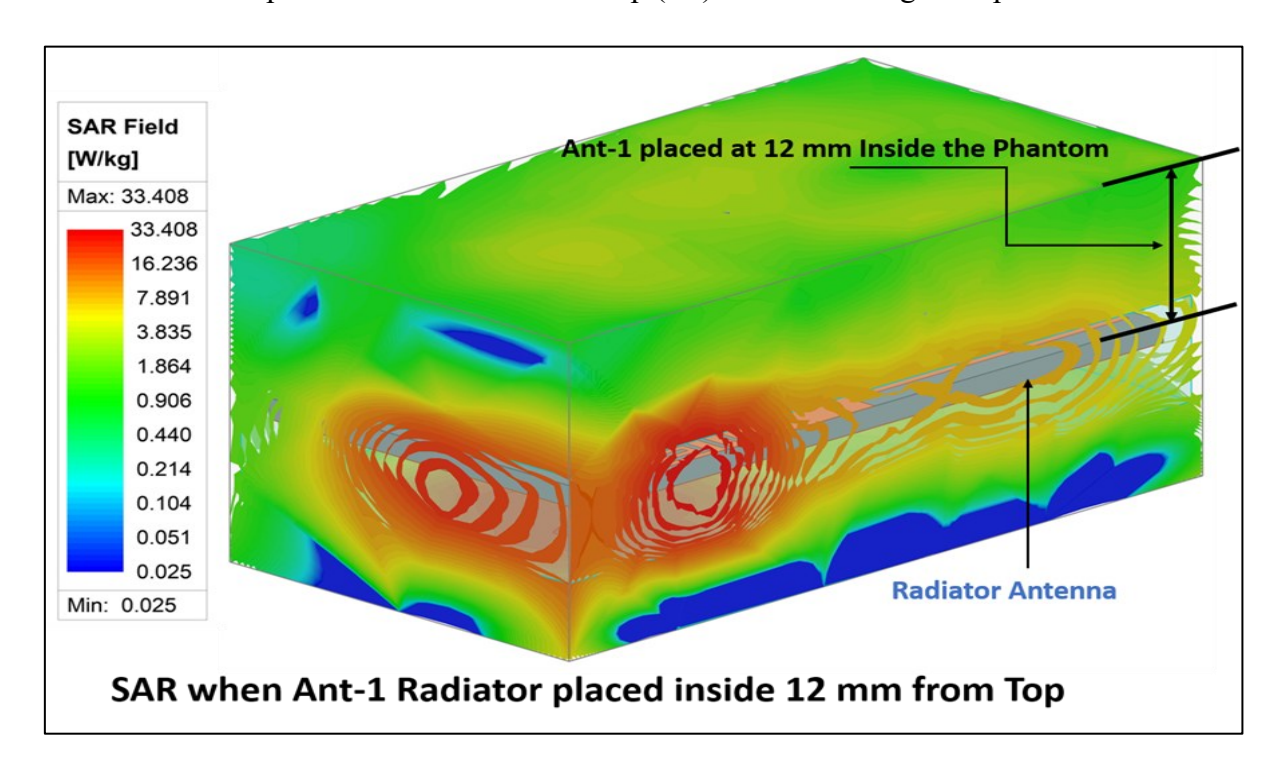


**Figure 8.** Ant-1 with a Mimicking Muscles Phantom Model and Ant-1 Inside the Muscle Phantom Model for Bio-Medical Applications.

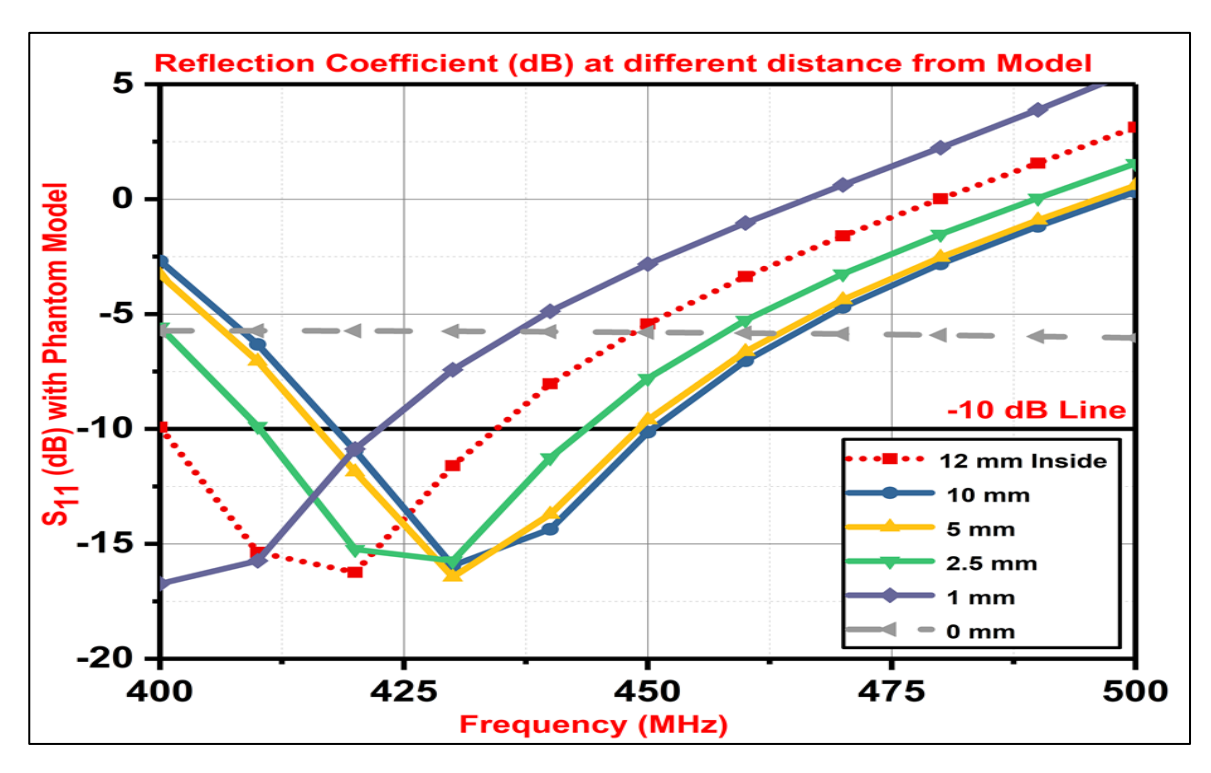


**Figure 9.** Parametric Analysis of Mimicking Muscles Phantom Model w.r.t Ant-1 Distance.

Figure 10 shows the fabricated prototype antenna (Ant-1) with the actual sensor RFM RO2021 for 433 MHz biomedical applications. Figure 10(a) shows the top side of the fabricated antenna, and Figure 10(b) shows the bottom side of the fabricated antenna (Ant-1) with the mounted sensor.

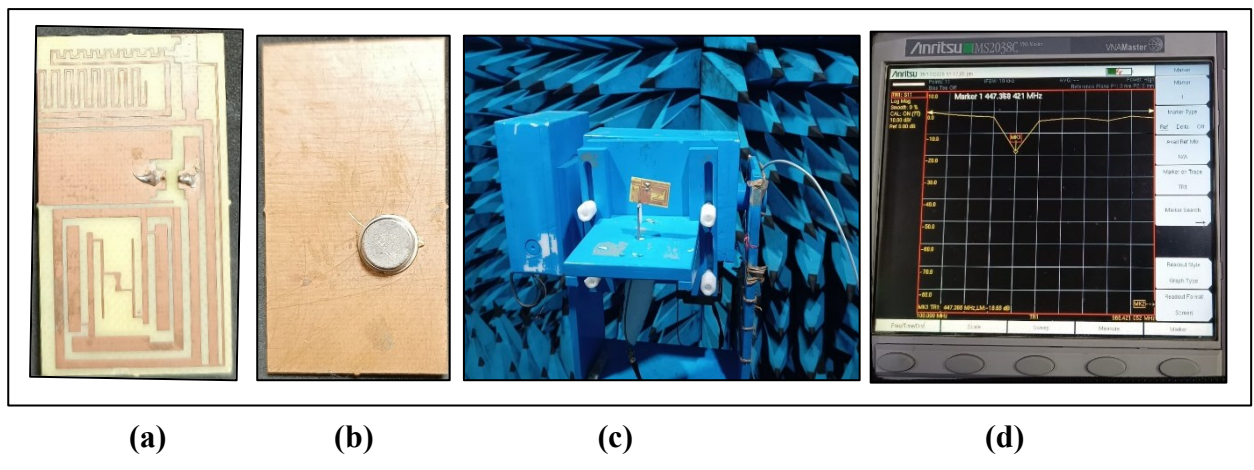


**Figure 10.** Fabricated Prototype Antenna (Ant-1) for Bio-Medical Application: (a) Top Side-Radiating Patch, (b) Bottom Side-Ground Plane with Sensor, (c) Antenna Measurement Setup, and (d) VNA Measurement.

# 4. Conclusion

In this paper, we investigate two distinct types of antennas: Ant-1 (microstrip patch antenna) and Ant-2 (helical antenna), utilizing high-frequency structured simulation (HFSS) software for biomedical applications, specifically for animal implantable and ingestible applications. Both antennas were analyzed using a similar sensor. Antenna performance was assessed based on reflection coefficient, voltage standing wave ratio (VSWR), current distribution, and radiation pattern, both with and without a phantom model. Ant-1 demonstrated superior performance compared to Ant-2, as detailed in Table 2 of the results and analysis section. The analyzed results indicate that Ant-1 operates within an acceptable range, both with and without a muscle phantom model, in the 433 MHz ISM band. Measurements taken with a vector network analyzer (model no. MS2038C) revealed a slight shift in the resonant frequency to 447.38 MHz. This study underscores the necessity of precise optimization steps for biomedical applications and concludes that this prototype is suitable for animal implantable and ingestible biomedical applications.

# Acknowledgements

We would like to acknowledge the aid support of DST No: SCP/2022/000802 and (CARS-99) R&D/SA/DRDO/ECE/2023-24/02/465. The authors would like sincerely thank to IIT BHU Varanasi Lab members and staff supports

### References

- [1] Omboni, Stefano, Raj S. Padwal, Tourkiah Alessa, Béla Benczúr, Beverly B. Green, Ilona Hubbard, Kazuomi Kario et al. "The worldwide impact of telemedicine during COVID-19: current evidence and recommendations for the future." Connected health 1 (2022): 7.
- [2] Khan, Tayyaba, MuhibUr Rahman, Adeel Akram, Yasar Amin, and Hannu Tenhunen. "A low-cost CPW-fed multiband frequency reconfigurable antenna for wireless applications." Electronics 8, no. 8 (2019): 900.
- [3] Riaz, Sharjeel, Mansoor Khan, Umer Javed, and Xiongwen Zhao. "A miniaturized frequency reconfigurable patch antenna for IoT applications." Wireless Personal Communications (2022): 1-11.

- [4] Kokkonen, Mikko, Mikko Nelo, Henrikki Liimatainen, Jonne Ukkola, Nuutti Tervo, Sami Myllymäki, Jari Juuti, and Heli Jantunen. "Wood-based composite materials for ultralight lens antennas in 6G systems." Materials Advances 3, no. 3 (2022): 1687-1694.
- [5] Kiourti, Asimina, and Konstantina S. Nikita. "A review of in-body biotelemetry devices: Implantables, ingestibles, and injectables." IEEE Transactions on Biomedical Engineering 64, no. 7 (2017): 1422-1430.
- [6] Gurain, G. "Miniature microwave biosensors." IEEE Microw. Mag 16, no. 4 (2015): 71-86.
- [7] Pang, Changhyun, Chanseok Lee, and Kahp-Yang Suh. "Recent advances in flexible sensors for wearable and implantable devices." Journal of Applied Polymer Science 130, no. 3 (2013): 1429-1441.
- [8] Zheng, Ya-Li, Xiao-Rong Ding, Carmen Chung Yan Poon, Benny Ping Lai Lo, Heye Zhang, Xiao-Lin Zhou, Guang-Zhong Yang, Ni Zhao, and Yuan-Ting Zhang. "Unobtrusive sensing and wearable devices for health informatics." IEEE transactions on biomedical engineering 61, no. 5 (2014): 1538-1554.
- [9] Govindan, Thennarasi, Sandeep Kumar Palaniswamy, Malathi Kanagasabai, Sachin Kumar, Rajesh Agarwal, Rajkishor Kumar, and Damodar Panigrahy. "Design and analysis of a conformal mimo ingestible bolus sensor antenna for wireless capsule endoscopy for animal husbandry." IEEE Sensors Journal 23, no. 22 (2023): 28150-28158.
- [10] Benaissa, Said, Denys Nikolayev, Günter Vermeeren, Kenneth Deprez, Jasper Goethals, Bart Sonck, Frank AM Tuyttens, Luc Martens, David Plets, and Wout Joseph. "Design and experimental validation of a multiband conformal patch antenna for animalingestible bolus applications." IEEE Transactions on Antennas and Propagation 71, no. 8 (2023): 6365-6377.
- [11] Saadat, Waqar, Sumit A. Raurale, Gareth A. Conway, and John McAllister. "Wearable antennas for human identification at 2.45 GHz." IEEE Transactions on Antennas and Propagation 70, no. 1 (2021): 17-26.
- [12] Sato, Shigeru, Hitoshi Mizuguchi, Kazunori Ito, Kentaro Ikuta, Atushi Kimura, and Keiji Okada. "Development and testing of a radio transmission pH measurement system for continuous monitoring of ruminal pH in cows." Preventive veterinary medicine 103, no. 4 (2012): 274-279.

- [13] Eihvalde, Indra, Daina Kairisa, and Ilga Sematovica. "Long-term continuous monitoring of ruminal ph and temperature for dairy cows with indwelling and wireless data transmitting unit." Parameters 3555, no. 4525 (2016): 4829.
- [14] Gallagher, M. W., B. C. Santos, and D. C. Malocha. "Wireless wideband SAW sensorantenna design." In 2010 IEEE International Frequency Control Symposium, IEEE, (2010): 291-296.
- [15] Kumar, Rupesh, and Nirupama Mandal. "SAW Sensor Basics on Material, Antenna, and Applications: A Review." IEEE Sensors Journal 24, no. 5 (2024): 5713-5731.
- [16] Saroj, Abhishek Kumar, and Jamshed Aslam Ansari. "A reconfigurable multiband rhombic shaped microstrip antenna for wireless smart applications." International Journal of RF and Microwave Computer-Aided Engineering 30, no. 10 (2020): e22378.
- [17] Das, Soumyadeep, and Debasis Mitra. "A compact wideband flexible implantable slot antenna design with enhanced gain." IEEE Transactions on Antennas and Propagation 66, no. 8 (2018): 4309-4314.
- [18] Lee, Chien-Ming, Tzong-Chee Yo, Fu-Jhuan Huang, and Ching-Hsing Luo. "Bandwidth enhancement of planar inverted-F antenna for implantable biotelemetry." Microwave and Optical Technology Letters 51, no. 3 (2009): 749-752.
- [19] International Commission on Non-Ionizing Radiation Protection. "Guidelines for limiting exposure to electromagnetic fields (100 kHz to 300 GHz)." Health physics 118, no. 5 (2020): 483-524.
- [20] Chow, Eric Y., Chin-Lung Yang, and Pedro P. Irazoqui. "Wireless powering and propagation of radio frequencies through tissue." In Wireless Power Transfer, River Publishers, (2022): 301-335.
- [21] Kiourti, Asimina, and Konstantina S. Nikita. "A review of in-body biotelemetry devices: Implantables, ingestibles, and injectables." IEEE Transactions on Biomedical Engineering 64, no. 7 (2017): 1422-1430.